

Limits on the Performance of RF-Over-Fiber Links and Their Impact on Device Design

Charles H. Cox III, *Fellow, IEEE*, Edward I. Ackerman, *Senior Member, IEEE*, Gary E. Betts, *Member, IEEE*, and Joelle L. Prince, *Member, IEEE*

Invited Paper

Abstract—This paper is divided into two major parts. Following a brief introduction that establishes some definitions and assumptions, Section II updates our earlier study on the limits of the RF performance of optical links. Section III reviews progress since our 1997 review paper in the development of devices enabling link performance closer to these limits, including (but not limited to): 1) cascade lasers that permit broad-band direct modulation links with gain >0 dB; 2) injection-locked edge- and surface-emitting lasers at 1300 and 1550 nm with modulation frequency responses as great as 40 GHz; 3) modulators with improved performance, especially electroabsorption modulators that now have switching voltages as low as 0.36 V, or handle optical powers as great as 60 mW, or have bandwidths as great as 50 GHz (but not all three of these in one device yet); and 4) high-speed photodetectors with high saturation currents, e.g., a 20-GHz device with a saturation current of 90 mA and a 55-GHz device with saturation at 50 mA. We conclude in Section IV by summarizing the component developments necessary for higher performance RF-over-fiber links, i.e.: 1) semiconductor lasers (for direct modulation) that have higher slope efficiency and bandwidth and lower relative intensity noise (RIN) at reasonable bias current levels; 2) continuous wave (CW) lasers (for external modulation) with higher fiber-coupled power and lower RIN; 3) higher frequency lower loss external modulators with more linear transfer functions and lower V_{π} that can withstand larger CW optical powers; and 4) photodetectors with higher responsivity and bandwidth that respond linearly even when illuminated by greater average optical powers.

Index Terms—Future development, microwave photonics, reviews, technological forecasting.

I. INTRODUCTION

THE USE of optical links for the transmission of RF (analog) signals has continued to expand for more than 15 years. Perhaps the first widespread commercial application of analog optical links was the distribution of cable television (CATV) signals [1]. Although perhaps not as large in dollar sales, antenna remoting has been an important application in both commercial and military markets [2]. More recently, RF-over-fiber has been a growing application area for analog optical links [3].

Although it is common to refer collectively to such links as “RF” or “analog” optical links, this may lead to confusion when

the modulation consists of a digital signal that is modulated onto an RF carrier. Thus, it is perhaps more technically precise to define analog optical links as ones where the optical modulation depth is sufficiently small that we may use incremental or small-signal models of the various link devices. This is in contrast to “digital” optical links in which the optical modulation depth approaches 100%.

It has become common practice to measure the RF performance of optical links using the same parameters that are used to characterize other RF components [4]. In this paper, we focus on the primary ones, i.e.: 1) gain; 2) bandwidth; 3) noise figure (NF); and 4) spur-free dynamic range (SFDR).

Initially naive “link design” merely consisted of connecting the optical output of a diode laser to the input of a photodiode. However, the RF performance of such links was often modest at best, and terrible at worst; typically one would obtain from such a “design” a link loss of 40 dB and an NF of 50 dB, which severely limited the applications of such links.

To address these shortcomings there has grown up over the last 15 years or so the field of link design, which is closely related to, but distinct from, device design. A dramatic early example of the power of link design was the work of Cox *et al.* [5], who were able to achieve RF gain from link components that otherwise would have resulted in substantial link loss.

There have been at least two other outgrowths of link design. One outgrowth has been to highlight which device parameters will have an impact on link parameters and to quantify that impact. For example, reductions in the threshold current of a diode laser have no impact on link gain, whereas increases in slope efficiency have a major impact. (One may, of course, want to reduce the threshold current for other reasons.)

Another outgrowth of link design has been the ability to establish the limits on link performance [6]. Such limits have proven useful in providing a “calibration” on the progress in link performance that has been made relative to the ultimate progress that at least theoretically should be achievable.

In this paper, we begin in Section II by reviewing—and where necessary updating—the limits on the RF performance of analog optical links. We also present the state-of-the-art in link performance that has been achieved for the four principal analog figures-of-merit, i.e.: 1) gain; 2) NF; and 3) SFDR. Clearly, improvements in link performance are highly dependent on improvements in device performance. Hence, Section III reviews the state-of-the-art in the principal

Manuscript received July 18, 2005; revised October 22, 2005.

The authors are with Photonic Systems Inc., Billerica, MA 01821 USA (e-mail: eackerman@photonicsinc.com).

Digital Object Identifier 10.1109/TMTT.2005.863818

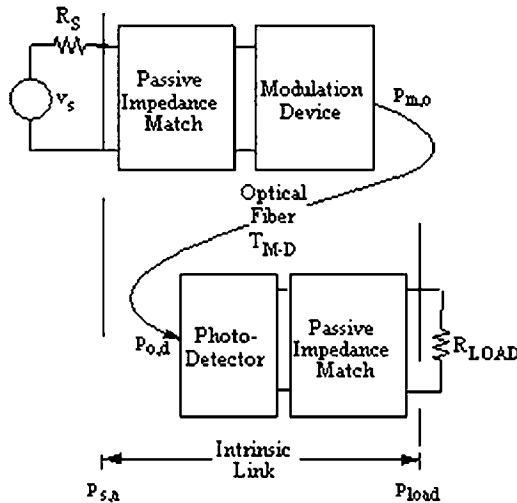


Fig. 1. Block diagram of the intrinsic intensity-modulation/direct-detection link (after [7]).

link components, i.e.: 1) laser; 2) external modulator; and 3) photodetector.

The implementation of a link involves several design tradeoffs. To keep the discussion of this paper to manageable proportions, we have limited its scope in the following three ways.

- 1) We assume single-mode fiber links of short (e.g., less than 1 km) length, such that dispersion and nonlinearity in the fiber have negligible effect on the link's performance.
- 2) We discuss only the *intrinsic* link. As shown in Fig. 1 (after [7]), the intrinsic link consists of an RF-to-optical modulation device, an optical-to-RF demodulation device, and a short (less than 1 km) length of fiber to connect the two. Since some of the RF definitions require impedance matching, we also include the passive components necessary to accomplish this in the definition of an intrinsic link. It is important to note that we explicitly exclude any amplification, either RF or optical, from the definition of the intrinsic link. The exclusion of optical amplifiers makes sense given assumption 1) because, in short spans of fiber, the optical intensity does not degrade to an extent that warrants amplifying it prior to the detector. The exclusion of electronic amplifiers avoids their obscuring effects (i.e., added noise and nonlinear distortion), thereby increasing the visibility for the interaction between device and link parameters.
- 3) We limit the discussion to direct-detection links and, therefore, to intensity-modulation links because no other type of modulation can be recovered using direct detection. Readers interested in an overview of links using other types of modulation and detection are referred to reviews such as that of Seeds [8] on coherent-detection links.

II. PRINCIPAL LINK PARAMETERS AND LIMITS ON THEIR PERFORMANCE

A. Gain and Bandwidth

We begin by examining link gain because of its central role when the link is viewed from both the “outside” and the “inside.”

From the “outside,” i.e., when the link is viewed as a component within a larger system—link gain is an important parameter in setting the overall performance of the system. Gain is also important from the “inside,” i.e., when one is dealing with the design tradeoffs among the parameters of the intrinsic link.

Of the several definitions of RF gain that are commonly used to characterize RF components, the transducer power gain has been found to be the most useful for optical links. Hence, we define the intrinsic link gain to be the transducer power gain of an amplifierless optical link. Since this is the only definition of gain we use in this paper, we simply refer to this quantity as gain. Note from the definition that there is no requirement that the gain be greater than 1. Thus, we use the term “gain” in the general sense wherein gains less than 1 represent loss.

It has been shown [7] that the gain g_i can be expressed simply as

$$g_i = s_{md}^2 r_d^2 \quad (1)$$

where s_{md} is the slope efficiency of the modulation device (with dimensions of watts per ampere) and r_d is the responsivity of the detection device (with dimensions of amperes per watt). In (1), the input resistance of the modulation device has been assumed to equal the link's output load resistance.

There are no fundamental limits that set a minimum or maximum link gain. However, a practical limit on gain is set by the limits of slope efficiency and responsivity. For links in which one is constrained to direct modulation of a single conventional diode laser and a p-i-n photodiode, it can be shown that the link gain is limited to be less than or equal to 1 in the case where the laser input resistance and detector load resistance are equal [7]. Such links will have RF loss so that, from a system perspective, they operate like an attenuator (although we will see from a noise-figure perspective that such a link is actually worse than an attenuator).

If, however, optically linking the two opto-electronic devices results in a product of modulation device slope efficiency and detector responsivity exceeding 1, then the link gain will be greater than 1, i.e., the link will act as an RF amplifier. Whereas in principle it is possible to achieve positive link gain by imbuing either opto-electronic device with a sufficiently efficient response, to the authors' knowledge, positive gain from an analog optical link has been demonstrated only by increasing the slope efficiency of the modulation device.

There are at least two reasons for this. One reason stems from the desire to achieve low NF. As is discussed in Section II-B, increasing the slope efficiency of the RF-to-optical modulation device is more effective at reducing the link's NF than increasing the responsivity of the optical-to-RF demodulation device (photodetector). The second reason comes from the desire to achieve high SFDR. As is discussed in Section II-C, the highly nonlinear behavior of currently known photodetection devices having responsivities corresponding to more than one electron generated per incoming photon—i.e., avalanche photodiodes—severely limits the achievable SFDR [9]. Consequently, in the remainder of this paper, we will assume a p-i-n photodiode is used for the optical-to-RF demodulation

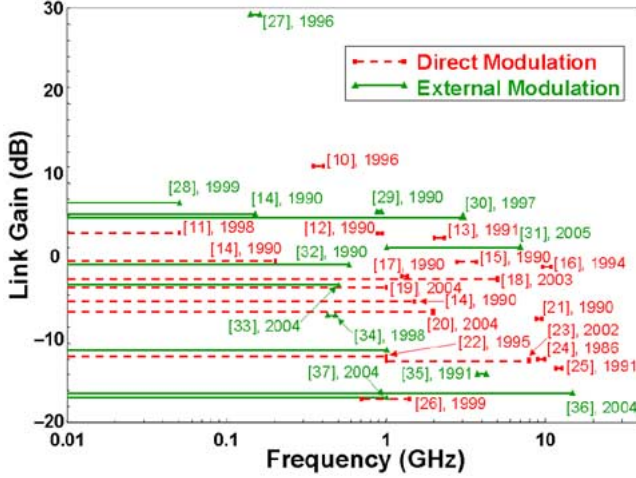


Fig. 2. Published gains of intrinsic (i.e., amplifierless) analog optical links versus frequency.

device—which has a responsivity that limits the gain of conventional direct-modulation/direct-detection links to less than 1—and focus on techniques for increased slope efficiency in the RF-to-optical modulation device.

Fig. 2 shows the best link gain results (i.e., those with gain > -20 dB) that have been achieved to date [10]–[37]. Eleven of these results [11], [18], [23], [26], [29]–[31], [33], [34], [36], [37] were reported since the submission of our 1997 review paper [4], and three of these new results [11], [18], [31] are significant in ways discussed further below.

Techniques for improved slope efficiency of direct modulation include the cascade laser [11], [18] and the gain lever laser [38]. However, to date, only the cascade laser has been used to construct a direct modulation link with positive link gain. The first demonstration of a broad-bandwidth direct-modulation link with positive gain was by Cox *et al.* [11] who constructed a cascade laser from discrete diode lasers. Since then other groups have demonstrated various approaches to fabricating monolithic versions of a cascade laser [18], [39], but to date none of these devices are available commercially.

Unlike a directly modulated laser, for which slope efficiency is a native parameter of the device, the slope efficiency of an external modulator is a derived parameter [7]. For example, a Mach–Zehnder modulator biased at quadrature has a slope efficiency of

$$s_{mzi} = \frac{\pi P_I T_{ff} R_s}{2V_\pi} \quad (2)$$

where P_I is the continuous wave (CW) laser power into the modulator, T_{ff} is the fiber-to-fiber transmission of the modulator, R_s is the impedance of the source, and V_π is the modulator's on–off switching voltage. Equation (2) makes clear the basis for the commonly employed techniques for improving the slope efficiency of external modulation: increasing the laser's output optical power and reducing the modulator's switching voltage. When both of these techniques are used in the same link, the performance can be quite impressive; e.g., using a Mach–Zehnder modulator with a measured 6-GHz V_π of 1.81 V to modulate 187 mW of laser power, Ackerman *et al.*

recently demonstrated a link with broad-bandwidth positive gain up to 8 GHz [31]. Higher gain requires a laser with higher optical power, a low-loss modulator that can withstand this higher power, and a high-speed detector that can handle higher powers without saturating.

In general, improving the slope efficiency is a broad-bandwidth way of increasing the link gain. In applications where only a bandpass frequency response is required, it is possible to trade some of the excess bandwidth for increased response (i.e., slope efficiency and/or responsivity) within the frequency range of interest. The reason for this is that the impedance of virtually all known opto-electronic link components is different from the common characteristic system impedances: 75 Ω for TV and 50 Ω for everything else. There is, however, a tradeoff between the degree of impedance match—and, hence, the degree of link gain improvement—and the bandwidth over which this match can be achieved. This tradeoff has been expressed analytically by the Bode-Fano limit [7], [40].

Narrow-band impedance matching was combined with the broad-bandwidth techniques for improved slope efficiency listed above for an external modulation link to yield a link with a gain of 31 dB and a 3-dB bandwidth between 140–160 MHz [27], which, to our knowledge, is the highest published gain for an amplifierless link.

To summarize the manner in which the desire for greater analog link gains affects (or ought to affect) opto-electronic component design, we have shown that the slope efficiency of a single directly modulated laser cannot yield a link gain of greater than 0 dB. By contrast, the slope efficiency of an external modulator can theoretically be increased without bound to yield very high gains (as shown in Fig. 2) by reducing V_π and increasing P_I , although some practical limitations on the optical power do come into play. To enable greater direct and external modulation link gains, the various devices should then be designed with the following criteria in mind:

- *directly modulated lasers*: highest possible s_I ;
- *CW lasers for external modulation*: highest possible P_I ;
- *external modulators*: lowest possible V_π ; largest possible T_{ff} (up to its maximum value of 1); capability of withstanding highest possible P_I ;
- *photodetectors*: highest possible r_d (in both direct and external modulation links); capability of withstanding highest possible optical power (external modulation links only);

and, to enable greater bandwidth, the directly modulated lasers, external modulators, and photodetectors all need to be designed for high speed.

B. NF

An intrinsic link's NF is defined as the degradation of signal-to-noise ratio (SNR) when its input noise is the thermal noise generated at $T_0 = 290$ K [41]. This input thermal noise is amplified (or attenuated) by the link's intrinsic gain (or loss) g_i . Therefore,

$$\text{NF} \equiv 10 \cdot \log \left[\frac{n_{\text{out}}}{kT_0 B \cdot g_i} \right] \quad (3)$$

where the input thermal noise is the product of k (Boltzmann's constant), T_0 (290 K), and B (the instantaneous bandwidth of the electronic receiver, sometimes called the "resolution bandwidth" or "noise bandwidth"). Since the output noise term n_{out} is also proportional to B , the NF is independent of B .

If g_i is large enough that the amplified input thermal noise makes the dominant contribution to the total noise at the link output, then there is virtually no degradation in SNR from the link's input to its output and, consequently, its NF approaches 0 dB. This is obviously the absolute lower limit to the NF, and is difficult to realize in actual intrinsic fiber-optic links because of several other contributions to the output noise. Techniques for minimizing the NF stem from an understanding of all the sources of noise added by components in the link, and from knowing which of these sources of noise are completely unavoidable versus which ones can be mitigated in various ways.

There are two unavoidable sources of added thermal noise in a link. First, since the impedance of any modulator or semiconductor laser has some ohmic component, it generates thermal noise, as does the resistive portion of any circuit interfacing this device to the link input. Depending on this exact circuit configuration, some or all of this thermal noise will modulate the light and reach the link output just as the link's input thermal noise does, setting a new lower limit to the link NF that is greater than 0 dB. How much greater depends on several factors that have been documented elsewhere [42]. Unfortunately, very few links have been demonstrated in which either the link's input thermal noise or the thermal noise generated by the modulation device and its interface circuit dominates the link's total output noise.

The second unavoidable additional contribution to the total output thermal noise from an intrinsic link is the thermal noise generated in the photodetector circuit. This noise is usually roughly equal in amplitude to the link's input thermal noise. Therefore, if the intrinsic link has loss rather than gain, then the thermal noise generated in the photodetector circuit, rather than the attenuated input and modulation device thermal noises, will dominate the total thermal noise at the output of the link. In this case, the minimum possible SNR degradation from link input to link output is equal to $10 \cdot \log(1/g_i)$, which has been named the passive attenuation limit to the fiber-optic link NF because a passive attenuator's NF equals its loss [27]. Taking into account only the input thermal noise and these two unavoidable sources of added thermal noise, one finds the absolute lower limit to link the NF

$$\text{NF} = 10 \log \left[1 + \text{constant} + \frac{1}{g_i} \right] \quad (4)$$

where the unquantified "constant" expresses the effect of the first unavoidable source of added thermal noise arising in the modulation device circuit (discussed above) and the $1/g_i$ term quantifies the effect of the second unavoidable source of added thermal noise (discussed here). Note that even at frequencies where the first source is negligible, the second source of noise causes a link to have worse NF than an attenuator with equivalent loss. For example, an attenuator with loss approaching 0 dB will also have ~ 0 dB NF, whereas (4) dictates that a link with 0 dB loss will have an NF of at least 3 dB.

Even in low-loss or high-gain analog fiber-optic links for which the three terms in the brackets of (4) sum to a small number, two additional sources of added noise typically dominate the output noise and, therefore, a great deal of effort has been expended in trying to minimize them. First, the noise of the optical source, which is quantified by the term relative intensity noise (RIN), is detected along with the signal. Second, the statistical nature of the photodetection process itself results in shot noise. Like the thermal noise generated in the detection circuit, these sources of noise have amplitudes that are not directly related to the link gain. Therefore, since the link's NF is the ratio between its output noise and its amplified input thermal noise [see (3)], the RIN and shot noise terms in the NF equation are both inversely proportional to g_i . Specifically,

$$\text{NF} = 10 \log \left[1 + \text{constant} + \frac{1}{g_i} + \frac{\langle I_D \rangle^2 \text{RIN} R_S}{k T_0 g_i} + \frac{2q \langle I_D \rangle R_S}{k T_0 g_i} \right] \quad (5)$$

for a link in which the load presented to the photodetector is simply the output impedance of the link, i.e., without a "matching resistor" in the detector package—which has been assumed to equal the RF source resistance R_S . The only as-yet undefined parameters in (3) are the average photodetector current term $\langle I_D \rangle$ appearing in both the RIN- and shot noise-determined terms (the fourth and fifth addends within the brackets, respectively), and the electronic charge q that appears only in the shot noise term.

It is clear from (5) that the most obvious way to reduce NF is to increase g_i . Not all methods for increasing g_i are equally effective in reducing NF, however, because some of these methods also affect the magnitude of other terms in (5). For example, one of the common techniques for increasing the gain of an external modulation link—increasing the average optical power—also increases the effect of RIN and, hence, has no effect on the RIN-determined term in the NF equation. Additionally, increasing the link gain through adjustments to the circuit that interfaces the photodetector to the link's output port will generally have no effect upon either the RIN- or the shot noise-determined terms because such changes will affect how well the circuit couples these noise currents to the link output to the exact same extent as they affect how well it couples the signal photocurrent to the link output. These facts are easier to understand if we substitute the expression for g_i in the case of a Mach-Zehnder modulator-based external modulation link (for example) into the final three terms of (5) as follows:

$$\text{NF} = 10 \log \left[1 + \text{constant} + \frac{4V_\pi^2}{\pi^2 r_d^2 T_{ff}^2 P_I^2 R_S^2} + \frac{V_\pi^2 \text{RIN}}{\pi^2 k T_0 R_S} + \frac{4qV_\pi^2}{\pi^2 k T_0 r_d T_{ff} P_I R_S} \right] \quad (6)$$

To derive (6), it was also necessary to use the I_D expression for a Mach-Zehnder modulator at its quadrature bias point, i.e.,

$$I_D = \frac{r_d T_{ff} P_I}{2} \quad (7)$$

Recall from (1) and (2) that increasing the product $r_d T_{ff} P_I$ and reducing V_π are equally effective techniques for increasing g_i ;

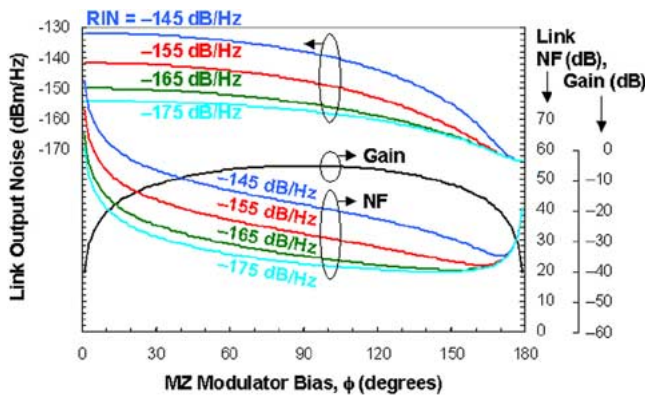


Fig. 3. Illustration of “low-biasing” technique for reducing the NF of an external modulation fiber-optic link that uses a Mach–Zehnder modulator. (Assumptions: $V_{\pi} = 3$ V, $I_D = 10$ mA at $\phi = 90^\circ$.) The link’s output noise (left axis) decreases more quickly than its gain (right axis), causing the optimum NF (right axis) to occur at a bias point between 90° – 180° .

notice from (6), however, that the latter technique (reducing V_{π}) is a more effective means of reducing NF than is the former. This is a distinction that is important when techniques are discussed for improving the link’s dynamic range.

Interestingly, it also sometimes turns out that, when attempting to improve g_i by impedance matching to the modulation device, the matching circuit design that maximizes g_i differs from the one that minimizes NF; one such situation was demonstrated in [42].

Besides increasing g_i , there is another way to reduce the link’s NF that is especially effective in links where the NF is RIN dominated. This technique, which was discovered independently by three groups in 1993 [43]–[45] has become known as “low biasing” an external modulator. The benefits of this technique are easiest to quantify in the case of a Mach–Zehnder external modulator in a linear electrooptic material like lithium niobate because its transfer function—and, therefore, its slope efficiency, as well as the link’s gain g_i and the average photocurrent I_D —can be expressed as simple functions of its dc-bias voltage V_M . Fig. 3 shows, for specific assumed photonic component values, the effect of the low-biasing technique on the NF of a Mach–Zehnder modulator-based external modulation link.

From the curves in Fig. 3 showing the intrinsic link gain (g_i) and the total output noise from the link, it is evident that the noise initially decreases more quickly than the signal as the modulator bias ϕ (where $\phi = 180^\circ \cdot V_M/V_{\pi} = \pi V_M/V_{\pi}$) is increased from 90° toward the light-extinguishing bias of 180° . At some optimum low-biasing point between 90° – 180° that depends on component parameters such as the laser RIN, the link’s NF is minimized. If the bias point is moved further toward 180° , the signal gain begins to decrease more quickly than the noise and, therefore, the NF begins to increase relative to its value at the optimum low-biasing point.

As is explained further in Section II-C, a modulator produces no second-order distortion only when biased where g_i is maximum (e.g., at $\phi = 90^\circ$ for a Mach–Zehnder modulator). Therefore, the low-biasing technique for reducing NF has an adverse effect on the link’s second-order distortion-limited dynamic range such that it tends not to be employed, except

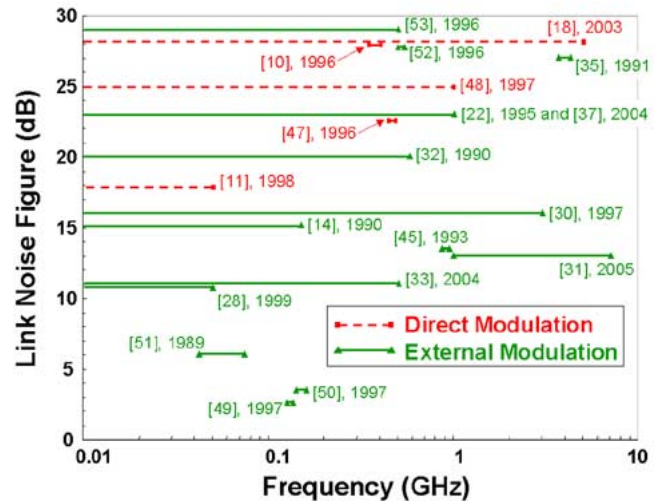


Fig. 4. Published NFs of intrinsic (i.e., amplifierless) analog optical links versus frequency.

in links with bandwidths of less than one octave in which all second-order distortion products fall out of band.

An additional way to reduce the NF in links where the NF is RIN dominated is to use one of several external modulation link architectures that use a balanced differential photodetector configuration to cancel the CW laser’s RIN. In the most conventional of these architectures, the two outputs from a quadrature-biased ($\phi = 90^\circ$) Mach–Zehnder modulator in which an optical directional coupler rather than a y-branch combiner produces the necessary interferometry and are connected via equal-length optical fibers to the two detectors. Since the two modulated outputs from the Mach–Zehnder modulator are complementary—i.e., 180° out-of-phase with one another—subtracting them in the differential detector configuration doubles the output signal current (thereby increasing g_i) while canceling the common-mode component, which is the laser’s RIN [30], [46].

Using one of the methods discussed here may sufficiently reduce the NF either such that no pre-amplifier is required to meet the system NF requirement or such that the gain that this pre-amplifier needs to have is not so large that the input second- or third-order intercept powers are reduced to the point where the link’s dynamic-range specification is unachievable.

Fig. 4 shows the best link NF results (i.e., those with NF < 30 dB) that have been achieved to date [10], [11], [14], [18], [22], [28], [30]–[33], [35], [37], [45], [47]–[53]. To achieve lower analog link NF, the various devices should be designed with the following criteria in mind:

- *directly modulated lasers*: all the criteria for high gain plus the lowest possible RIN at a bias current that enables high-speed operation, but does not yield a large value of I_D ;
- *CW lasers for external modulation*: all the criteria for high gain plus the lowest possible RIN;
- *external modulators*: all the criteria for high gain, but the most important is low V_{π} ; of secondary importance is largest T_{ff} and the capability of withstanding the highest possible optical power P_I ;

- *photodetectors*: highest possible r_d (both direct and external modulation links, same as the gain goal), capability of withstanding highest possible optical power (external modulation links only, same as the gain goal).

Not surprisingly, this set of criteria includes the set of device design criteria for high link gain given in Section II-A.

C. Dynamic Range

The dynamic range is uniquely important among link performance measures in that it is the only one that generally cannot be improved by adding an amplifier before or after the link.

We quantify the dynamic range as the two-tone SFDR. This is the SNR of one fundamental frequency at the link output when the link input consists of two equal-power fundamental frequencies at a power level that produces intermodulation distortion products with output powers equal to the output noise.

We are primarily concerned with the third-order SFDR. The third-order intermodulation frequencies are $2f_1 \pm f_2$ and $2f_2 \pm f_1$, where f_1 and f_2 are the fundamental input frequencies. The reason for the concern with the third-order products is that, in any system, the $2f_i - f_j$ frequencies may appear within the system bandwidth. The second-order SFDR is only important for systems whose bandwidth is more than one octave because the second-order intermodulation products $f_1 \pm f_2$ will fall outside the passband of a suboctave system.

In the following discussion, we separate links into two categories: “broad-band” and “suboctave.” Broad-band indicates that both second- and third-order distortion products are minimized, whereas suboctave indicates that only third-order distortion is minimized. (This refers to the ultimate application target of the link, but not to the experimental link itself. There are several examples of experimental links that have a 3-dB bandwidth spanning several octaves, but that are operated in such a way that only third-order distortion is minimized.) A link using a Mach–Zehnder external modulator can be operated in either a broad-band or suboctave mode. For example, if this modulator is biased exactly at the quadrature point of the modulator’s optical power versus voltage transfer function, all even-order distortion products are cancelled. The second-order SFDR is then very large and we consider this a broad-band link. If this same modulator is low biased to achieve better link NF [43]–[45], the second-order distortion becomes large (typically reducing second-order SFDR to approximately 60 dB in a 1-Hz noise bandwidth) and we consider the link a suboctave link.

The SFDR depends on the noise bandwidth because the noise bandwidth affects the output noise level. The functional dependence of the SFDR on the noise bandwidth depends on the relationship of intermodulation output power to fundamental input power. For standard links, the third-order distortion varies as the cube of the input RF power, which leads to an SFDR that depends on noise bandwidth to the $2/3$ power. For second-order distortion, the intermodulation products vary as the square of the input electrical power and, thus, the second-order SFDR depends on the noise bandwidth to the $1/2$ power. If a link is “linearized” by using a modulator or electrical circuit that cancels the dominant nonlinearity, the relationship can change so that there is a steeper dependence of intermodulation power on input power; the impact of this is that, for a linearized link, the

third-order SFDR will depend on the $4/5$ power of the noise bandwidth. In order to compare linearized and standard links on the same basis, we will pick a fixed noise bandwidth and compute the SFDR.

As was stated in Section I, this paper is concerned with intensity-modulation/direct-detection links, and this is the only type of link for which we discuss results below. Coherent analog links have also been investigated [8], [54]. Initially these were considered for systems where there was very low received power, and their performance was low compared to direct-detection links. Coherent-detection links can have SFDR comparable to direct detection links if the received power is sufficiently large. Links with SFDR up to 115 dB · Hz^{2/3} at frequencies up to 15 GHz have been reported [55]–[57]. Although we do not discuss these further, it should be noted that coherent links have advanced in performance along with the more common direct-detection links.

The absolute maximum achievable SFDR, which occurs in the total absence of distortion, is the SNR [7]; therefore, we briefly discuss what limits the maximum SNR of an intensity-modulation/direct-detection link. It is often assumed, usually to facilitate analysis, that a link is shot-noise limited, in which case the SNR can be made arbitrarily large by arbitrarily increasing the optical power—at least in principle.

For intensity-modulation links, the residual intensity fluctuations at the photodetector, with no signal applied to the modulation device, clearly will limit the minimum depth of signal modulation that can be conveyed by the link. Consequently, it is intuitively clear that some combination of thermal noise, shot noise, and RIN imposes a limit on the SNR. To formalize this limit, consider first a hypothetical photodetector that detects a signal modulating an equally hypothetical RIN-free optical carrier such that thermal noise generated in the detection circuit imposes the only upper limit upon the SNR. The photodiode modulation current i_d is related to the average detector current I_D by the optical modulation depth m viz.

$$i_d = mI_D. \quad (8)$$

The maximum $m = 1$; consequently, the maximum SNR under thermal noise-limited detection is simply

$$\text{SNR}_{\max} = 10 \log \left(\frac{1}{2} I_D^2 R_S \right) - 10 \log(kT_0). \quad (9)$$

Next, consider the maximum SNR limit set by shot noise by itself (in the hypothetical absence of thermal noise and RIN) as follows:

$$\begin{aligned} \text{SNR}_{\max} &= 10 \log \left(\frac{1}{2} I_D^2 R_S \right) - 10 \log(2qI_D R_S) \\ &= 6 \text{ dB} - 10 \log \left(\frac{I_D}{q} \right). \end{aligned} \quad (10)$$

Finally, the maximum SNR in the RIN-limited case (thermal or shot noise both hypothetically zero) is

$$\begin{aligned} \text{SNR}_{\max} &= 10 \log \left(\frac{1}{2} I_D^2 R_S \right) - 10 \log(I_D^2 \text{RIN} R_S) \\ &= -3 \text{ dB} - \text{RIN}(\text{in decibels}). \end{aligned} \quad (11)$$

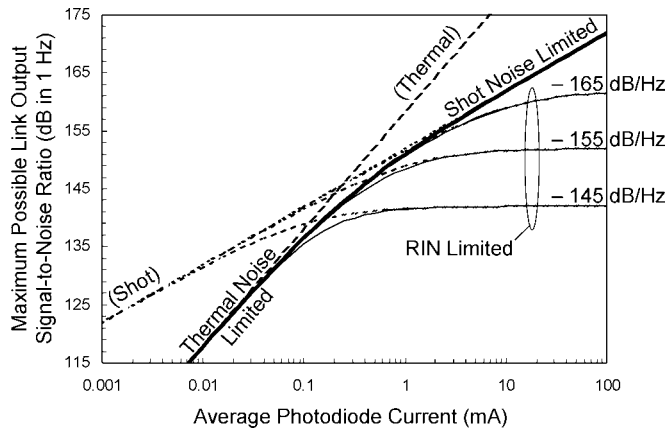


Fig. 5. Plot of the SNR versus average photodiode current for thermal noise-limited, shot noise-limited, and three cases of RIN-limited detection.

Fig. 5 shows these limits to SNR_{\max} as a function of I_D with three typical values of RIN used as a parameter. It is clear from this figure that the maximum SNR is poor for low values of I_D , but improves quickly as I_D is increased. However, for larger values of I_D , the laser's RIN imposes an SNR limit that cannot be exceeded by increasing I_D any further. Only for very low values of RIN can the very best situation be approximated, i.e., the shot noise limit shown by the upper rightmost extent of the heavy solid curve in Fig. 5 that represents the absolute physical limit to the link's output SNR for a given average photodiode current I_D .

To relate the above discussion of SNR_{\max} to an RF link's dynamic range, recall that the SFDR is defined as the highest SNR for which the intermodulation terms are equal to the noise floor. However, for an ideal modulation device with a strictly linear transfer function, there are no intermodulation terms, thus the maximum SFDR is the SNR.

If a modulator or directly modulated laser can be made to be almost perfectly linear, the resulting SFDR will be exceedingly large. An external modulator with a perfectly linear transfer function would generate no distortion products until the RF input voltage (peak) reaches half of the on-off voltage. For such a modulator, even an on-off voltage of only 0.3 V (sufficiently low to enable an NF of ~ 4 dB assuming a reasonable average photocurrent of ~ 10 mA if the RIN is negligibly low) would generate no distortion products until the input signal power reaches $(1/2) \cdot (V_{\pi}/2)^2 \div 50 \Omega$ or -6.5 dBm. This corresponds to an SFDR of $(-6.5 \text{ dBm} - [-174 \text{ dBm/Hz} + 4 \text{ dB}])$, or $163.5 \text{ dB} \cdot \text{Hz}$. However, according to (11), to realize this SFDR we also require a laser with a RIN of less than -166.5 dB/Hz , which is consistent with the low-RIN assumption used to calculate the NF.

In practical links, a maximum SNR of $> 155 \text{ dB} \cdot \text{Hz}$ can be readily achieved [58]. However, the nonlinearity of the modulator (or laser in the case of direct modulation) and of the photodetector limit the SFDR to a much smaller value than the SNR because intermodulation products appear above the noise floor at modulation depths much smaller than 1. A quantitative analysis of the nonlinearity can become quite lengthy because the connection to physical device parameters is different for each

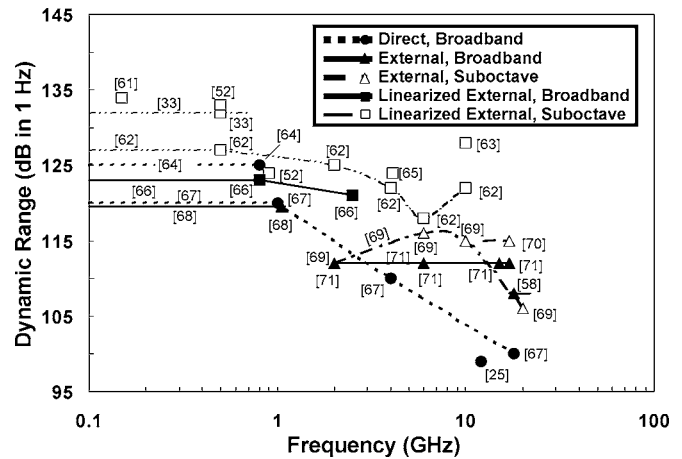


Fig. 6. Analog-link third-order SFDR versus frequency in a 1-Hz noise bandwidth. Points represent measured performance of specific links reported in the literature. Lines represent interpolated or extrapolated performance of specific links.

different type of modulation device. A more detailed discussion of dynamic range and linearization is found in [59].

In past discussions on the limits to analog link performance (e.g., [6] and [60]), the point has been made that lowering the V_{π} of a modulator to improve the link's NF reduces the link's SFDR as the NF approaches a value limited by input thermal noise and that there is, therefore, some value of V_{π} that yields an optimum NF-SFDR tradeoff. This assertion is relevant in a region of NF that only has been reached at low frequencies (< 200 MHz) as of yet. As modulators and lasers improve, however, this tradeoff will become more important.

With the above background, Fig. 6 shows published SFDRs in a 1-Hz noise bandwidth [25], [33], [52], [58], [61]–[71]. The y -axis scale corresponds numerically to the commonly used bandwidth scaling quantities $\text{dB} \cdot \text{Hz}^{2/3}$ and $\text{dB} \cdot \text{Hz}^{4/5}$.

Direct modulation links [25], [64], [67] have large SFDR (up to $125 \text{ dB} \cdot \text{Hz}^{2/3}$ [64]) at < 1 GHz, but suffer from significantly decreasing SFDR as the frequency increases [67]. This is due to properties inherent to the laser, namely that as the operating frequency gets closer to the relaxation oscillation resonance, the distortion worsens [72]. These links are broad-band because second-order distortion is fairly low (second-order SFDR of $102 \text{ dB} \cdot \text{Hz}^{1/2}$ at < 1 GHz was demonstrated in [64] simultaneously with the high third-order SFDR). However, this second-order distortion is still too large for CATV transmission (the largest multioctave optical analog link application) and, therefore, for this application second-order linearization needs to be applied electronically.

External modulation links can have high SFDR out to higher frequencies [58], [71]. Links using a standard Mach-Zehnder interferometric modulator do not have quite as high a third-order SFDR as directly modulated links below 1 GHz, but they are able to maintain a high SFDR out to a much higher frequency. The link in [71] achieved $112 \text{ dB} \cdot \text{Hz}^{2/3}$ from 2 to 17 GHz. Second-order distortion can be very low, limited by the detector, because the modulator can be biased so it creates zero second-order distortion. In this type of link, high optical power reaches the detector because the modulator is biased at a point where it transmits half of its maximum power. Large SFDRs

of $119.5 \text{ dB} \cdot \text{Hz}^{2/3}$ (third-order limited) and $126 \text{ dB} \cdot \text{Hz}^{1/2}$ (second-order limited) were achieved at frequencies up to 1 GHz in [68] by using a specially designed high-power detector. Electroabsorption modulators can also enable very high-frequency analog links [73], but typically they have not achieved as high an SFDR in this mode as the Mach–Zehnder because of limited optical power-handling ability.

Suboctave versions of links using the Mach–Zehnder modulator have demonstrated dynamic range of up to $115 \text{ dB} \cdot \text{Hz}^{2/3}$ at frequencies of up to 20 GHz [69], [70]. High SFDR is easier to achieve at high frequencies with a sub-octave link because the modulator can be biased closer to its off state so that only a small amount of optical power reaches the detector. This allows use of high laser power for high SFDR without requiring a high power detector.

Suboctave linearized modulators have produced the highest SFDR in a 1-Hz noise bandwidth. The highest performance has been demonstrated at low frequencies: $134 \text{ dB} \cdot \text{Hz}^{4/5}$ at 150 MHz [61], and $> 130 \text{ dB} \cdot \text{Hz}^{4/5}$ at frequencies up to 500 MHz [32], [52]. There is no fundamental problem with extending this linearized modulator SFDR to higher frequencies, but practical difficulties such as tighter manufacturing tolerances for cascaded modulators make it more difficult, and the nonlinearity of high-frequency detectors also becomes a factor limiting the link performance. The electroabsorption modulator has a bias point that gives minimum third-order distortion, which results in linearized performance with a very simple modulator. This type of modulator has generated some of the highest SFDRs at high frequency [62], [63], [65]: up to $128 \text{ dB} \cdot \text{Hz}^{4/5}$ at 10 GHz [63].

Broad-band linearized modulators are also possible, but it is harder to get high performance using them. One example that has been reported in a link is the linearized directional-coupler modulator [74], but experimental difficulties prevented it from achieving its full potential and limited its link's SFDR to $111 \text{ dB} \cdot \text{Hz}^{4/5}$. A technique using two wavelengths of light in a single Mach–Zehnder modulator resulted in a broad-band link with an SFDR of $121 \text{ dB} \cdot \text{Hz}^{4/5}$ up to 2.5 GHz [66].

Practical system noise bandwidths are much larger than 1 Hz. Since the linearized links' SFDRs have a steeper dependence on noise bandwidth than do those of standard links, the advantage shown in Fig. 6 is reduced as the bandwidth increases. To see how the picture changes as the bandwidth increases, the results of Fig. 6 were replotted in Fig. 7 using a noise bandwidth of 500 MHz. This is a rather extreme case in that most current systems have noise bandwidths less than one-tenth as large as this, but it may be representative of future high-performance systems. Fig. 7 shows that, for large noise bandwidth, the advantage of the linearized modulators is reduced substantially to the point where they have little advantage over standard modulators at frequencies $> 1 \text{ GHz}$, and are even beaten by the best direct modulation link below 1 GHz.

To achieve greater link SFDR, the various devices should be designed with the following criteria in mind:

- *directly modulated lasers*: all the criteria listed for high gain and low NF, plus as linear as possible a power-versus-current curve and a very high relaxation oscillation frequency;

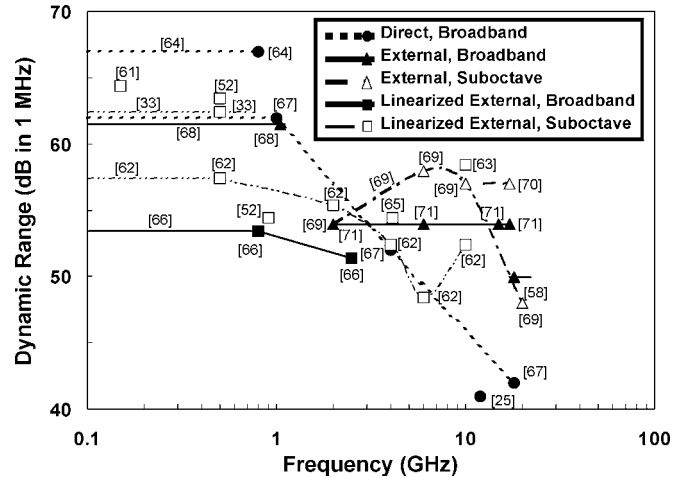


Fig. 7. Analog-link third-order SFDR versus frequency in a 500-MHz noise bandwidth.

- *CW lasers for external modulation*: highest possible P_I and lowest possible RIN (same as for the gain and NF goals);
- *external modulators*: all the criteria listed for high gain and low NF, plus as linear as possible a power-versus-voltage curve;
- *photodetectors*: all the criteria listed for high gain and low NF, plus as linear as possible an output current versus input power curve.

III. IMPACTS ON DEVICE DESIGN

A. Laser

1) *Lasers for Direct Modulation Links*: In Section II, it was established that the desire for high-frequency direct modulation links with high gain, low NF, and wide SFDR drives the need for semiconductor lasers that can be directly modulated at high speeds and with the greatest possible linearity and low RIN. Here, we discuss progress in the development of high-speed lasers since 1997.

Virtually all direct-modulation intensity-modulation/direct-detection links use diode lasers with one of two edge emitting laser cavity designs: Fabry–Perot (FP) or distributed feedback (DFB). Some low-performance links use light-emitting diodes. To date, vertical-cavity surface-emitting lasers (VCSELs) have only begun to have much impact on analog-link designs, at least partially because the majority of the efforts have been at $\sim 850 \text{ nm}$, where the VCSEL material and fabrication problems are more tractable, but fiber loss and chromatic dispersion are high. Recent efforts have demonstrated VCSELs at $\sim 1550 \text{ nm}$ with a modulation frequency response $> 40 \text{ GHz}$ [75].

The best direct intensity-modulation/direct-detection link gains are plotted versus frequency in Fig. 2 [10]–[26]. Note that most of the direct modulation-link gains fall below 0 dB. This is a simple consequence of conservation of energy, which limits the product of laser diode slope efficiency and photodetector slope efficiencies to be less than 1. As will be discussed further below, although the direct modulation-link gain is independent of average optical power, the gain is proportional to the square

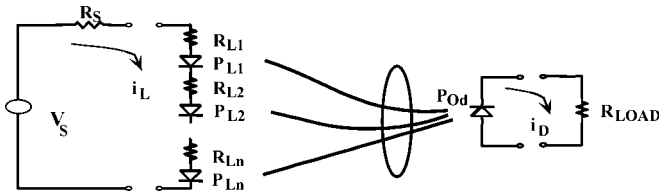


Fig. 8. Conceptual diagram of the cascade laser, wherein individual lasers are connected electrically in series and their optical outputs are coupled in parallel onto a photodetector (after [11]).

of the laser's fiber-coupled slope efficiency. Coupling its highly divergent diode-laser beam into the low-divergence mode of a fiber is relatively inefficient, making the single-mode fiber coupled slope efficiencies of commercially available devices typically 10%–65% of the diode-chip slope efficiency. The highest reported efficiency of butt coupling to a single mode fiber is 80% [76]. The fiber-coupled slope efficiencies of currently available diode lasers range from 0.1 to 0.32 W/A. Using the highest value of slope efficiency, and assuming a perfect detector responsivity (corresponding to one electron per 1550-nm photon) and that all other link losses are negligible, the link gain is -9.5 dB.

An obvious way to improve the gain of direct modulation links would be to use a type of semiconductor laser with higher laser-slope efficiency such as the gain-lever laser [38]. However, initial attempts to achieve high link gain using this laser have been unsuccessful. Further, the substantial nonlinearity of this laser's p versus i curve (as shown in [38]) suggests that its SFDR will be unacceptable for the majority of analog-link applications.

Another method, the cascade laser, has shown improvement in the performance of slope efficiency; see Fig. 8. This was first demonstrated by Cox *et al.* [11] who derived the fact that the slope efficiency of the cascade is simply the sum of the slope efficiencies of the individual lasers in the cascade. Cox *et al.* achieved a low-frequency slope efficiency of 1.89 W/A by cascading six discrete lasers [11]. Getty *et al.* later achieved a 5-GHz 3-dB bandwidth and a slope efficiency of 1.01 W/A with a three-stage InP segmented-ridge cascade laser [18].

The slope efficiencies achievable from cascade lasers should permit direct modulation links to enter the realm of performance that had heretofore only been attainable using the more costly external modulation link approach. Extension of the cascade laser to greater efficiencies or powers is, however, limited. Individual lasers of the cascade are short and have high series resistance; connecting these electrically in series results in still higher overall device series resistance. Keeping overall device resistance acceptable for modulation limits the total number of devices that can be cascaded.

A second method of improving link gain is to accept reduced bandwidth for increased link gain. Many antenna remoting and some CATV applications have used this approach. One way to make this tradeoff is to replace the conventional resistive (i.e., lossy) impedance-matching circuits with lossless (at least ideally) reactive impedance-matching circuits. Since the real part of the laser impedance is typically less than the 50- Ω source impedance and the photodetector impedance is typically greater

than the 50- Ω load impedance, it is possible to make the ratio of photodetector to modulation-device resistances more than compensate for the extent to which the product of the square of the slope efficiencies is shy of 1, thereby using the gains from impedance matching to completely overcome the electrooptical slope efficiency losses. Three of the direct modulation links whose results are plotted in Fig. 2 achieved link gain >0 dB using this method [10], [12], [13].

The maximum broad-band frequency response that has been demonstrated for a diode laser is 40 GHz. This high 3-dB bandwidth (defined with respect to the low-frequency response) was obtained by damping the laser's 22-GHz relaxation oscillation so that the gain rolled off very slowly above this frequency [77]. However, at frequencies near the relaxation oscillation frequency, a laser's noise and distortion increases, which, in turn, degrades the NF and SFDR around this frequency [72]. Therefore, the maximum *usable* bandwidth for direct modulation analog links can be considerably less than the maximum 3-dB bandwidth.

It has been shown that the relaxation resonance frequency is proportional to the square root of the average optical power [78]. To achieve the record 40-GHz response required operating the laser at a bias current 10–12 times greater than the minimum current for lasing. To achieve further bandwidth increases via simple increases in the optical power will be difficult because of the laser heating due to the higher bias current. Different diode-laser active-layer architectures, such as the multiple quantum-well structure employed in the 40-GHz laser in [77], have been analytically determined to be capable of achieving much higher bandwidths, but to date, the experimental demonstrations have not borne out the theory.

Another method for modulation bandwidth enhancement has been accomplished with optical injection-locked edge-emitting lasers [79] and VCSELs [75]. The enhancement for the injection-locked VCSEL was dramatic, causing the free-running laser resonance of 6 GHz to increase to >40 GHz.

For applications that only require a very narrow passband, another way of circumventing the present bandwidth limit of semiconductor lasers is by exploiting the enhanced modulation response at frequencies that are at or near the laser cavity round-trip time. Lau [80] used this technique to demonstrate modulation at 40 GHz, albeit with a 3-dB passband width of only 200 MHz.

The lists in Sections II-A–C summarizing component development goals all included a desire for directly modulated lasers with higher s_l such as the ones discussed above, but also mentioned the need for lower RIN and for a more linear transfer function; we are not aware of any study published since 1997 on improving these latter two characteristics.

2) *Lasers for External Modulation Links:* As explained in Section II, the gain of an external modulation link is proportional to the square of the CW optical power supplied by the laser. Optical sources with narrow output spectra, such as semiconductor, solid-state, and doped-fiber lasers, are appropriate choices for CW optical sources in external modulation links because their output power levels and RIN characteristics can enable the desired link gain and NF. At the 1550-nm wavelength that is currently of greatest commercial interest, however, no

TABLE I
COMMERCIAL OFF-THE-SHELF SINGLE-FREQUENCY LASERS AT $\lambda = 1550$ nm

Laser type (cw)	Fiber-coupled power (mW)	RIN (dB/Hz)
Semiconductor DFB	60	-160
Doped-fiber laser	150	< -175
Doped-fiber oscillator with doped-fiber post-amp	> 1,000	-160

solid-state sources are commercially available, leaving semiconductor and doped-fiber lasers as the strongest candidates for an external modulation link. An erbium-doped fiber oscillator followed by an erbium-doped fiber amplifier (EDFA) is an appropriate choice when very high optical powers are needed. The currently available values of optical power and RIN are listed in Table I for standard commercial off-the-shelf lasers.

Another factor that sometimes has to be considered when choosing a CW laser is the dc power it consumes. The dc power efficiency (the ratio of the optical output power to this dc input power) has traditionally only been a quoted specification for the semiconductor lasers that supply the optical pumps in solid-state and doped-fiber lasers. If RF links are going to be considered for use in power-starved platforms such as satellites and unmanned air vehicles, the dc power efficiency and volume will be factors that system designers will also consider when selecting a laser.

B. Modulator

In an external modulation analog link, the modulator often is the dominant factor in determining link performance. There are several characteristics of the modulator that are important (most of which were set forth and briefly discussed in Sections II-A–C): the voltage sensitivity, usually represented by V_π , the impedance, the optical loss, the optical power-handling capability, the linearity, and the environmental stability. Here, we further discuss these characteristics in the context of particular modulators; for a more detailed discussion, see [7] and [59].

There are three materials that have been used for most of the modulators reported in the literature and used in systems: lithium niobate, III–V semiconductors, and polymers. A variety of modulator designs can be built in each of these materials. The performance of a modulator is determined by the material, the modulator design, and the aggregate amount of effort that has been spent developing the modulator. We will look at one modulator design in each of these materials, choosing as examples the devices that have demonstrated the highest performance to date.

The most highly developed modulator is the Mach–Zehnder interferometric modulator in lithium niobate. This device has been investigated and engineered for 30 years and is in widespread commercial use. Lithium niobate is a very stable material and Ti-indiffusion offers a well-controlled method for making stable low-loss optical waveguides that can be coupled to single-mode fibers with low loss. The modulation mechanism is the linear electrooptic effect, which has only a small dependence on wavelength or temperature and will respond to frequencies >100 GHz. Typical fiber-to-fiber optical insertion

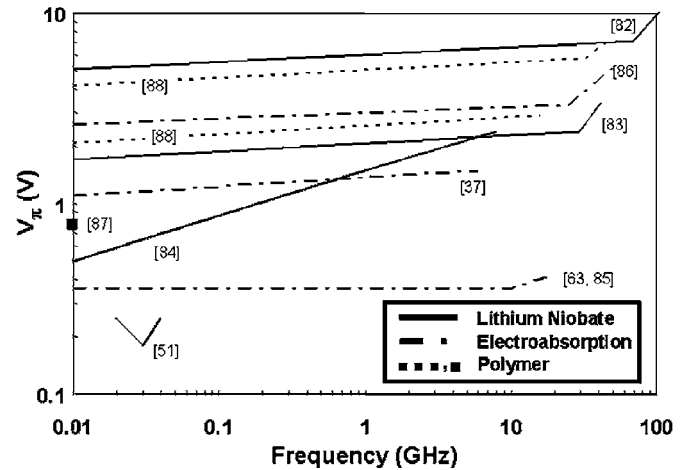


Fig. 9. Modulator V_π versus frequency. Lines (and, in one case, a single square) represent measured performance of specific modulators reported in the literature. A few state-of-the-art results are shown for each of the types of modulators discussed in this paper. Wavelengths are 1300–1550 nm and impedance is generally near 50 Ω for all these devices.

losses for these devices are 3–7 dB. Commercial versions of these modulators have passed the Telcordia qualification, which includes 10 000 h at 85 $^{\circ}\text{C}$ [81], and the devices will typically withstand temperatures up to 125 $^{\circ}\text{C}$ while operating. The ultimate upper limit to optical power handling is not known, but there have been several measurements with up to 500-mW input power at 1300–1550 nm with no serious problems.

The drawback of the lithium–niobate modulator for analog use is its poor sensitivity (at least relative to an ideal modulator) as represented by its unattractively large V_π . To achieve low NFs in analog links, a V_π of a few tenths of a volt is desirable. Fig. 9 shows the measured V_π as a function of frequency for the modulators with the lowest V_π at various frequencies; the solid lines are lithium–niobate Mach–Zehnder interferometric modulators (at 1300 or 1550 nm). This is the type of lithium–niobate modulator that has demonstrated the lowest V_π . At very low frequencies (<500 MHz), a lithium–niobate modulator can achieve $V_\pi < 1$ V with a bandpass impedance match; the record for this is $V_\pi = 0.18$ V at 30 MHz [51]. Lithium–niobate modulators can reach very high frequencies, but broad-band performance comes at the expense of high V_π . The widest bandwidth modulator of any type thus far reported is a lithium–niobate modulator with a 3-dB bandwidth of 70 GHz and a maximum measured frequency of 110 GHz [82]. This device has a low-frequency V_π of 5.1 V and is the highest V_π curve shown in Fig. 9. (There have been demonstrations of narrow-band modulation at higher frequencies than 110 GHz in various materials, but these generally do not have a V_π measurement and also all have 3-dB bandwidths <70 GHz.) Between the two extremes of low bandwidth with low V_π and high bandwidth with high V_π , there are intermediate choices. The two plotted in Fig. 9 [83], [84] represent the state-of-the-art.

The electroabsorption modulator built in III–V semiconductors is the next most developed type of modulator. This has been in development for 20 years. Many other modulator types, including the Mach–Zehnder interferometer, have been demonstrated in III–V semiconductors, but thus far, none has

achieved the low drive voltage and utility of the electroabsorption modulator.

The electroabsorption modulator is much more sensitive to temperature, wavelength, optical power, and device design than the lithium–niobate Mach–Zehnder interferometer. The sensitivity to wavelength and temperature is due to the basic operation mechanism of this type of modulator, which depends upon electric-field-induced changes in optical absorption near the band edge of the semiconductor. These issues have been engineered well enough for certain types of electroabsorption modulator—specifically one which is monolithically integrated with a laser [electroabsorption-modulated laser (EML)]—to be commercially viable. The dependence on device design is actually an advantage: there are more variables to control and optimize in an electroabsorption modulator than in a lithium–niobate modulator so performance is still improving rapidly.

There are three examples of an electroabsorption modulator shown in Fig. 9. The lowest voltage device has an equivalent V_π of only 0.36 V at dc and a 3-dB bandwidth >20 GHz [63], [85], making it the lowest voltage broad-band modulator of any type thus far reported. (Electroabsorption modulators do not have an unambiguous on and off voltage so an equivalent V_π is calculated by giving the V_π required for an interferometric modulator to have the same maximum slope of optical transmission versus voltage.) This modulator, however, has this low V_π only for optical power <2 mW. If the optical power is 24 mW, the V_π rises to 0.58 V at dc. An electroabsorption modulator can be designed for high power; one of the highest power devices can handle 60 mW, but its V_π at dc is 1.1 V [37]. Fiber-coupled insertion losses of these modulators are high—typically 10–20 dB. Electroabsorption modulators are capable of very high frequency operation, although there will be some tradeoff with voltage. A modulator operating up to 50 GHz had an equivalent dc V_π of 2.6 V [86]. The high switching voltage of this device relative to that of [63] does not necessarily completely represent a bandwidth-dependent effect; it also represents an advance in the state-of-the-art between [86] in 1997 and [63] in 2003.

Polymer modulators are the least mature technology of the three. Like lithium niobate, polymer modulators work via the linear electrooptic effect and, thus, the basic operation mechanism is capable of very high frequencies. Also like lithium niobate, the predominant modulator design is the Mach–Zehnder interferometric modulator. Most of the development effort has focused on the polymer material itself. A variety of host polymers and electrooptically active chromophore dopants have been investigated. Since the polymer material can be engineered for high electrooptic effect, the hope is that very low V_π can eventually be achieved. In general, though, the polymer materials with larger electrooptic effects are the least stable against temperature and optical power.

The polymer modulators plotted in Fig. 9 represent the lowest polymer V_π 's reported. These examples operate at 1300 or 1550 nm and have fiber-to-fiber optical losses of 6–10 dB. The lowest polymer modulator V_π reported is 0.78 V at dc [87]. This modulator had a broad-band electrode structure, but no high-frequency results were reported for it. This device had an estimated optical insertion loss of 6 dB and maximum power-handling ability of 20 mW. It used a low-temperature

polymer system that degraded if exposed to 75 °C for more than a few minutes. A somewhat more robust polymer modulator was reported in [88]. This achieved a dc V_π of 2.1 V in a 16-GHz device and 4.2 V in a device that operated up to 50 GHz. This device was able to withstand 1000 h at 60 °C. It also was limited to 20 mW of optical power. If V_π is compromised, a polymer modulator can be quite stable. For example, [89] reports a polymer modulator that withstood 2000 h at 100 °C and could handle 250 mW of optical power at 1300 nm; however, the V_π was 27 V at dc and its bandwidth, if measured, was not reported. It should be kept in mind that both the stability and the electrooptic effect of polymers are continually improving and the performance given here is just the current state of reported results.

As mentioned earlier, V_π is not the only critical parameter describing modulator performance in an analog link. The optical power output of the modulator, and its impedance, are also important. It is easy to combine V_π and impedance into a single measure expressing the modulator's sensitivity to RF power, but we choose to stay with the more familiar V_π in Fig. 9 because all these modulators had approximately 50- Ω impedance or were tested so that V_π could be reported in the 50- Ω environment.

When link gain is the performance measure of interest, the relevant modulator-related quantity is the slope efficiency s_m , as defined in (2) for a Mach–Zehnder modulator. In this case, V_π and optical power throughput ($P_I T_{ff}$) are weighted equally.

When the NF is the measure of interest, the relative importance of V_π and optical power will depend on which contribution to the output noise is most important. The relationships can be seen clearly in (6). If receiver thermal noise is the dominant noise source in the link, then the NF is inversely proportional to link gain and, therefore, proportional to $V_\pi^2 / (P_I T_{ff})^2$; thus, V_π and optical power are weighted equally. However, as discussed in Section II, if receiver noise is the dominant noise source, this indicates that the link is behaving like an attenuator, which is usually far from desirable. In the much more desirable scenario where link output noise is dominated by shot noise, the NF is proportional to $V_\pi^2 / P_I T_{ff}$ and, thus, V_π has more of an effect than optical power. Finally, if the link output noise is dominated by RIN, the NF is proportional to V_π^2 , and there is no optical power dependence at all. Thus, there are several relevant measures that combine optical power with V_π to express how the modulator affects link performance.

Another issue in evaluating the optical power output of the modulator is the relative importance of insertion loss and maximum power-handling ability. Insertion loss is important when the modulator's optical power-handling ability is larger than other limitations on optical power in the link. In this case, the insertion loss determines how powerful a laser must be used to achieve a given output power. Optical power-handling ability, however, is critical when it is low enough that it sets the limit on the optical power that may be used in a link. This is often the case for polymer and electroabsorption modulators.

It is clear from the above discussion that there are many ways to take into account the relative importance of V_π and optical power when evaluating the overall performance of a modulator. We have given the state-of-the-art for V_π in Fig. 9. To give an example of how the various modulators perform when optical

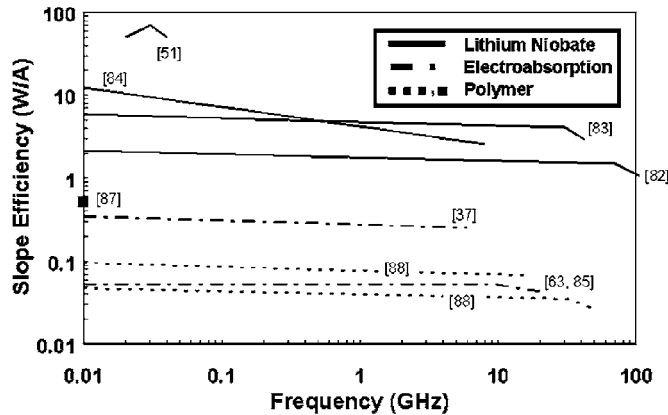


Fig. 10. Modulator slope efficiency versus frequency. Lines represent approximate calculations based on measured performance of specific modulators reported in literature.

power is also taken into account, we will choose the most extreme case, which is a link where the modulator power-handling ability sets the optical power level, and where the relevant performance parameter is the link gain. In this case, the slope efficiency s_m will be the appropriate performance measure. This is shown in Fig. 10 for most of the modulators represented in Fig. 9. The combination of large power handling and reasonable V_π gives the lithium–niobate modulator a much larger slope efficiency than the other types. If the power-handling ability of electroabsorption modulators can be brought up to be comparable to that of lithium–niobate modulators while preserving low V_π , they will overtake lithium–niobate modulators in slope efficiency. The importance of power handling can be seen in that the electroabsorption modulator with the highest slope efficiency is not the one with the lowest V_π [63], but instead the one with the highest power-handling ability [37].

C. Photodetector

In Section II, it was established that the desire for high-frequency direct and external modulation links with high gain, low NF, and wide SFDR drives the need for photodetectors that respond efficiently and linearly to light that is modulated by high-frequency analog signals. In the case of an external modulation links, whose performance is generally better for larger values of optical power, the importance of responding linearly to modulated light that has a large average value was also stressed as an important desired quality of the detector.

Our 1997 review paper [4] discussed the tradeoffs between responsivity, bandwidth, and power handling, including a comparison of surface and edge emitters in this regard. Since then, these issues have been treated in greater depth in other recent photodetector technology tutorials and reviews (e.g., [90] and [91]). Since 1997, it appears that the most significant change in the technology has been the advent of high-speed photodetectors with greater power-handling capability. Fig. 11, provided to us by Li and Campbell of The University of Texas at Austin [92], reviews the progress in the development of photodetectors demonstrating high saturation currents and 3-dB bandwidths between 100 MHz–100 GHz [92]–[100].¹

¹[Online]. Available: http://www.u2t.de/pdf/Datasheet_XPDV2020R&2020_V42.pdf

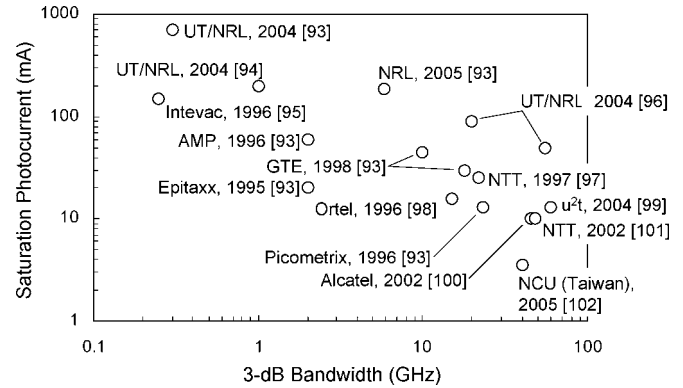


Fig. 11. Published optical power-handling capability of photodetectors versus RF frequency.

As previously stated, the future availability of high-speed detectors with greater and greater optical power-handling capability will enable external modulation links to have increased gain and reduced NF. The optical power-handling capability is an even more important factor in determining the achievable SFDR because it goes hand in hand with the device's linearity. In most conventional analog links—those that do not use a linearized modulator—the modulator's or directly modulated laser's nonlinearity dominates that of the link and thereby sets the limit on the link SFDR. It has been shown, however, that in links with linearized modulators, the detector's nonlinearity can set the upper limit on the SFDR. Therefore, if the need for modulators and directly modulated lasers with more linear transfer functions is fulfilled, detectors with greater linearity (and, therefore, higher power-handling capability) will be needed to reap the benefits of an improved link SFDR, as we have previously discussed [4].

IV. SUMMARY

In Section II, we have updated our earlier study [6] on the limits of the RF performance of optical links finding that the following component developments are necessary to enable links with better gain, NF, and SFDR:

- semiconductor lasers that have high slope efficiency and bandwidth and low RIN at reasonable bias current levels;
- CW lasers with high fiber-coupled power and low RIN;
- high-frequency low-loss external modulators with linear transfer functions and low V_π that can withstand large CW optical powers;
- photodetectors with high responsivity and bandwidth that respond linearly even when illuminated by large average optical power.

In Section III, we have discussed the progress since our 1997 review paper [4] in the development of devices addressing these needs, including, but not limited to, the following:

- cascaded semiconductor lasers [11], [18] that theoretically permit direct modulation links with gain >0 dB across broad RF bandwidths;
- injection-locked edge- and surface-emitting lasers at 1300 and 1550 nm that have been demonstrated with modulation frequency responses as great as 40 GHz [75];

- modulators with improved performance, especially electroabsorption modulators that now have switching voltages as low as 0.36 V [63], [85], or handle optical powers as great as 60 mW [37], or have bandwidths as great as 50 GHz [86];
- high-speed photodetectors with high saturation currents, e.g., a 20-GHz device with a saturation current of 90 mA and a 55-GHz device saturating at 50 mA [96].

The gap between what is theoretically possible and what can be experimentally demonstrated has narrowed considerably in the nine years since our last published review of the state-of-the-art, and prospects for further improvements look promising. We, therefore, conclude that another update to this review of RF-over-fiber technology will be warranted some time around the year 2010.

ACKNOWLEDGMENT

The authors thank Prof. W. Bridges, California Institute of Technology, Pasadena, for helpful discussions about laser RINs, and Dr. N. Li and Prof. J. Campbell, both with the University of Texas at Austin (at the time of this paper's writing), for the data plotted in Fig. 11.

REFERENCES

- [1] T. Darcie and G. Bodeep, "Lightwave subcarrier CATV transmission systems," *IEEE Trans. Microw. Theory Tech.*, vol. 38, no. 5, pp. 524–533, May 1990.
- [2] C. Cox, E. Ackerman, and G. Betts, "The role of photonic and electronic gain in the design of analog optical links," in *Proc. IEEE Avion. Fiber-Opt. Photon. Conf.*, Minneapolis, MN, 2005, pp. 71–72.
- [3] A. Seeds, "Microwave photonics," *IEEE Trans. Microw. Theory Tech.*, vol. 50, no. 3, pp. 877–887, Mar. 2002.
- [4] C. Cox, E. Ackerman, R. Helkey, and G. Betts, "Techniques and performance of intensity-modulation, direct-detection analog optical links," *IEEE Trans. Microw. Theory Tech.*, vol. 45, no. 8, pp. 1375–1383, Aug. 1997.
- [5] C. Cox, G. Betts, and L. Johnson, "An analytic and experimental comparison of direct and external modulation in analog fiber-optic links," *IEEE Trans. Microw. Theory Tech.*, vol. 38, no. 5, pp. 501–509, May 1990.
- [6] C. Cox and E. Ackerman, "Limits on the performance of analog optical links," in *Review of Radio Science 1996–1999*, W. R. Stone, Ed. Oxford, U.K.: Oxford Univ. Press, 1999, ch. 10.
- [7] C. Cox, *Analog Optical Links*. Cambridge, U.K.: Cambridge Univ. Press, 2004.
- [8] A. Seeds, "Optical transmission of microwaves," in *Review of Radio Science 1993–1996*, W. R. Stone, Ed. Oxford, U.K.: Oxford Univ. Press, 1996, ch. 14.
- [9] Y. Takahashi, K. Nagano, and Y. Takasaki, "Optical receiver for VHF multichannel video transmission," *IEEE J. Sel. Areas Commun.*, vol. 8, no. 7, pp. 1382–1386, Sep. 1990.
- [10] A. Goutzoulis, J. Zomp, and A. Johnson, "An eight-element, optically powered, directly modulated receive UHF fiber-optic manifold," *Microw. J.*, vol. 39, pp. 74–86, Feb. 1996.
- [11] C. Cox, H. Roussell, R. Ram, and R. Helkey, "Broadband, directly modulated analog fiber optic link with positive intrinsic gain and reduced noise figure," in *Proc. IEEE Int. Microw. Photon. Top. Meeting*, Princeton, NJ, 1998, pp. 157–160.
- [12] E. Ackerman, D. Kasemset, S. Wanuga, D. Hogue, and J. Komiak, "A high-gain directly modulated L-band microwave optical link," in *IEEE MTT-S Int. Microw. Symp. Dig.*, Dallas, TX, 1990, pp. 153–155.
- [13] S. Wanuga, E. Ackerman, D. Kasemset, J. Komiak, D. Peters, R. Scotti, W. MacDonald, and J. Gates, "Integrated microwave optoelectronic transceivers for lightweight fiber optic harnesses and remote microwave signal transmission," in *Proc. Gov. Microelectron. Applicat. Conf.*, Las Vegas, NV, 1991, pp. 79–81.
- [14] C. Cox, D. Tsang, L. Johnson, and G. Betts, "Low-loss analog fiber-optic links," in *IEEE MTT-S Int. Microw. Symp. Dig.*, Dallas, TX, 1990, pp. 157–160.
- [15] D. Huff and J. Anthes, "Optoelectronic isolator for microwave applications," *IEEE Trans. Microw. Theory Tech.*, vol. 38, no. 5, pp. 571–576, May 1990.
- [16] E. Ackerman, J. MacDonald, J. Prince, J. Sowers, R. Webb, and M. Dorsett, "Lowest-loss X-band photonic link for military and commercial applications," in *Proc. Gov. Microelectron. Applicat. Conf.*, Las Vegas, NV, 1994, pp. 102–104.
- [17] D. Kasemset, E. Ackerman, S. Wanuga, P. Herczfeld, and A. Daryoush, "A comparison of alternative modulation techniques for microwave optical links," *Proc. SPIE-Int. Soc. Opt. Eng.*, vol. 1371, pp. 104–114, Sep. 1990.
- [18] J. Getty, L. Johansson, E. Skogen, and L. Coldren, "1.55- μm bipolar cascade segmented ridge lasers," *IEEE J. Sel. Topics Quantum Electron.*, vol. 9, no. 5, pp. 1138–1145, Sep/Oct. 2003.
- [19] L. Chrostowski, C. Chang, and C. Chang-Hasnain, "Injection-locked 1.55- μm tunable VCSEL for uncooled WDM transmitter applications," *IEEE Photon. Technol. Lett.*, vol. 16, no. 3, pp. 888–890, Mar. 2004.
- [20] H. Sung, T. Jung, D. Tishinin, K. Liou, W. Tsang, and M. Wu, "Optical injection-locked gain-lever distributed Bragg reflector lasers with enhanced RF performance," in *Proc. IEEE Int. Microw. Photon. Topical Meeting*, Ogunquit, ME, 2004, pp. 225–228.
- [21] H. Blauvelt, D. Huff, G. Stern, and I. Newberg, "Reduced insertion loss of X-band RF fiber-optic links," *IEEE Trans. Microw. Theory Tech.*, vol. 38, no. 5, pp. 662–664, May 1990.
- [22] C. Sun, G. Anderson, R. Orazi, M. Berry, S. Pappert, and M. Shadaram, "Phase and amplitude stability of broad-band analog fiber optic links," *Proc. SPIE-Int. Soc. Opt. Eng.*, vol. 2560, pp. 50–56, Feb. 1995.
- [23] C. Carlsson, H. Marinsson, and A. Larsson, "High performance microwave link using a multimode VCSEL and a high-bandwidth multimode fiber," in *Proc. IEEE Int. Microw. Photon. Topical Meeting*, Long Beach, CA, 2002, pp. 81–84.
- [24] M. de La Chapelle, J. Gulick, and H. Hsu, "Analysis of low loss impedance matched fiber-optic transceivers for microwave signal transmission," *Proc. SPIE-Int. Soc. Opt. Eng.*, vol. 716, pp. 120–125, Sep. 1986.
- [25] E. Ackerman, D. Kasemset, S. Wanuga, R. Boudreau, J. Schlafer, and R. Lauer, "A low-loss Ku-band directly modulated fiber optic link," *IEEE Photon. Technol. Lett.*, vol. 3, no. 2, pp. 185–187, Feb. 1991.
- [26] P. Myslinski, C. Szubert, R. Misner, and J. Lee, "High-performance, low-cost fiber optic delay lines for analog applications," *Microw. Opt. Technol. Lett.*, vol. 20, pp. 173–177, Feb. 1999.
- [27] C. Cox, E. Ackerman, and G. Betts, "Relationship between gain and noise figure of an optical analog link," in *IEEE MTT-S Int. Microw. Symp. Dig.*, San Francisco, CA, 1996, pp. 1551–1554.
- [28] W. Burns, M. Howerton, and R. Moeller, "Broadband unamplified optical link with RF gain," in *Proc. Photon. Syst. Antenna Applicat. Conf.*, Monterey, CA, 1999, pp. 44–48.
- [29] E. Ackerman, D. Kasemset, S. Wanuga, and S. Chinn, "High-gain, wide dynamic range L-band externally modulated fiber-optic link," *Electron. Lett.*, vol. 26, pp. 1339–1341, Aug. 1990.
- [30] K. Williams, L. Nichols, and R. Esmen, "Externally-modulated 3 GHz fiber-optic link utilizing high current and balanced detection," *Electron. Lett.*, vol. 33, pp. 1327–1328, Jul. 1997.
- [31] E. Ackerman, G. Betts, W. Burns, J. Prince, M. Regan, H. Roussell, and C. Cox, "Low noise figure, wide bandwidth analog optical link," in *Proc. IEEE Int. Microw. Photon. Top. Meeting*, Seoul, Korea, 2005, pp. 325–328.
- [32] C. Cox, G. Betts, and A. Yee, "Incrementally lossless, broad-bandwidth analog fiber-optic link," in *Proc. IEEE LEOS Summer Top. Meeting*, Monterey, CA, 1990, pp. 15–16.
- [33] Y. Zhuang, W. Chang, and P. Yu, "Peripheral-coupled-waveguide MQW electroabsorption modulator for near transparency and high spurious free dynamic range RF fiber-optic link," *IEEE Photon. Technol. Lett.*, vol. 16, no. 9, pp. 2033–2035, Sep. 2004.
- [34] J. Prince, H. Roussell, E. Ackerman, and R. Knowlton, "Low-cost, high performance optoelectronic components for antenna remoting," *Opt. Quantum Electron.*, vol. 30, pp. 1051–1063, Dec. 1998.
- [35] W. Glomb, J. Farina, and S. Merritt, "Minimum noise figure microwave transmission system," in *Proc. Gov. Microelectron. Applicat. Conf.*, Las Vegas, NV, 1991, pp. 25–28.
- [36] S. O'Brien, H. Foulk, H. Gebretsadik, N. Frateschi, W. Choi, A. Bond, S. Robertson, and R. Jambunathan, "Highly integrated 1.55 μm analog transmitter for high speed (15 GHz), high dynamic range analog transmission," in *Proc. IEEE Int. Microw. Photon. Topical Meeting*, Ogunquit, ME, 2004, pp. 281–284.

- [37] J. Chen, Y. Wu, W. Chen, I. Shubin, A. Clawson, W. Chang, and P. Yu, "High-power intrastep quantum well electroabsorption modulator using single-sided large optical cavity waveguide," *IEEE Photon. Technol. Lett.*, vol. 16, no. 2, pp. 440–442, Feb. 2004.
- [38] K. Vahala, M. Newkirk, and T. Chen, "The optical gain lever: A novel gain mechanism in the direct modulation of quantum well semiconductor lasers," *Appl. Phys. Lett.*, vol. 54, pp. 2506–2508, Jun. 1989.
- [39] T. Knodl, M. Golling, A. Straub, R. Jager, R. Michalzik, and K. Ebeling, "Multistage bipolar cascade vertical-cavity surface-emitting lasers: Theory and experiment," *IEEE J. Sel. Topics Quantum Electron.*, vol. 9, no. 5, pp. 1406–1414, Sep./Oct. 2003.
- [40] R. Fano, "Theoretical limitations on the broad-band matching of arbitrary impedances," *J. Franklin Inst.*, vol. 249, pp. 57–84, and 139–154, Jan. 1950.
- [41] H. Haus *et al.*, "IRE standards on methods of measuring noise in linear twoports, 1959," *Proc. IRE*, vol. 48, no. 1, pp. 60–68, Jan. 1959.
- [42] E. Ackerman, C. Cox, G. Betts, H. Roussell, K. Ray, and F. O'Donnell, "Input impedance conditions for minimizing the noise figure of an analog optical link," *IEEE Trans. Microw. Theory Tech.*, vol. 46, no. 12, pp. 2025–2031, Dec. 1998.
- [43] G. Betts and F. O'Donnell, "Improvements in passive, low-noise-figure optical links," in *Proc. Photon. Syst. Antenna Applicat. Conf.*, Monterey, CA, 1993, pp. 41–43.
- [44] M. Farwell, W. Chang, and D. Huber, "Increased linear dynamic range by low biasing the Mach-Zehnder modulator," *IEEE Photon. Technol. Lett.*, vol. 5, no. 7, pp. 779–782, Jul. 1993.
- [45] E. Ackerman, S. Wanuga, D. Kasemset, A. Daryoush, and N. Samant, "Maximum dynamic range operation of a microwave external modulation fiber-optic link," *IEEE Trans. Microw. Theory Tech.*, vol. 41, no. 8, pp. 1299–1306, Aug. 1993.
- [46] E. Ackerman, S. Wanuga, J. MacDonald, and J. Prince, "Balanced receiver external modulation fiber-optic link architecture with reduced noise figure," in *IEEE MTT-S Int. Microw. Symp. Dig.*, Atlanta, GA, 1993, pp. 723–726.
- [47] R. Helkey, H. Roussell, C. Cox, and G. Betts, "Fabry-Perot laser high linearity analog optical links," in *Proc. IEEE Int. Microw. Photon. Top. Meeting*, Kyoto, Japan, 1996, pp. 233–236.
- [48] H. Roussell, R. Helkey, G. Betts, and C. Cox, "Effect of optical feedback on high dynamic range Fabry-Perot optical links," *IEEE Photon. Technol. Lett.*, vol. 9, no. 1, pp. 106–108, Jan. 1997.
- [49] E. Ackerman and C. Cox, "Explanation of the lossless passive match limit," in *Proc. Photon. Syst. Antenna Applicat. Conf.*, Monterey, CA, 1997, pp. 34–39.
- [50] E. Ackerman, C. Cox, G. Betts, H. Roussell, K. Ray, and F. O'Donnell, "Input impedance conditions for minimizing the noise figure of an analog optical link," in *IEEE MTT-S Int. Microw. Symp. Dig.*, Denver, CO, 1997, pp. 237–240.
- [51] G. Betts, L. Johnson, and C. Cox, "High-sensitivity lumped-element bandpass modulators in LiNbO₃," *J. Lightw. Technol.*, vol. 7, no. 12, pp. 2078–2083, Dec. 1989.
- [52] G. Betts and F. O'Donnell, "Microwave analog optical links using sub-octave linearized modulators," *IEEE Photon. Technol. Lett.*, vol. 8, no. 9, pp. 1273–1275, Sep. 1996.
- [53] R. Helkey, H. Roussell, C. Cox, M. Aoki, and H. Sano, "Octave bandwidth analog link with a monolithic laser/electroabsorption modulator," in *Proc. Integr. Photon. Res. Conf.*, 1996, pp. 217–219.
- [54] R. Kalman, J. Fan, and L. Kazovsky, "Dynamic range of coherent analog fiber-optic links," *J. Lightw. Technol.*, vol. 12, no. 7, pp. 1263–1276, Jul. 1994.
- [55] S. Datta and S. Forrest, "A 16-GHz linear analog heterodyne RF optical link employing a WIRNA receiver," *IEEE Photon. Technol. Lett.*, vol. 17, no. 4, pp. 890–892, Apr. 2005.
- [56] D. Sabido, M. Tabara, T. Fong, C. Lu, and L. Kazovsky, "Improving the dynamic range of a coherent AM analog optical link using a cascaded linearized modulator," *IEEE Photon. Technol. Lett.*, vol. 7, no. 7, pp. 813–815, Jul. 1995.
- [57] M. LaGasse and S. Thaniyavarn, "Bias-free high-dynamic-range phase-modulated fiber-optic link," *IEEE Photon. Technol. Lett.*, vol. 9, no. 5, pp. 681–683, May 1997.
- [58] G. Betts, C. Cox, and K. Ray, "20 GHz optical analog link using an external modulator," *IEEE Photon. Technol. Lett.*, vol. 2, no. 12, pp. 923–925, Dec. 1990.
- [59] G. Betts, "LiNbO₃ external modulators and their use in high performance analog links," in *RF Photonic Technology in Optical Fiber Links*, W. Chang, Ed. Cambridge, U.K.: Cambridge Univ. Press, 2002, ch. 4.
- [60] E. Ackerman and C. Cox, "Trade-offs between the noise figure and dynamic range of an analog optical link," in *Proc. Photon. Syst. Antenna Applicat. Conf.*, Monterey, CA, 2000, pp. 18–23.
- [61] G. Betts, F. O'Donnell, K. Ray, D. Lewis, D. Bossi, K. Kissa, and G. Drake, "Reflective linearized modulator," in *Proc. Integr. Photon. Res. Conf.*, 1996, pp. 626–629.
- [62] L. Johansson, J. Getty, Y. Akulova, G. Fish, and L. Coldren, "Sampled-grating DBR laser-based analog optical transmitters," *J. Lightw. Technol.*, vol. 21, no. 12, pp. 2968–2976, Dec. 2003.
- [63] B. Liu, J. Shim, Y. Chiu, A. Keating, J. Piprek, and J. Bowers, "Analog characterization of low-voltage MQW traveling-wave electroabsorption modulators," *J. Lightw. Technol.*, vol. 21, no. 12, pp. 3011–3019, Dec. 2003.
- [64] S. Pappert, C. Sun, R. Orazi, and T. Weiner, "Photonic link technology for shipboard RF signal distribution," in *Proc. SPIE-Int. Soc. Opt. Eng.*, vol. 3463, 1998, pp. 123–134.
- [65] R. Welstand, S. Pappert, C. Sun, J. Zhu, Y. Liu, and P. Yu, "Dual-function electroabsorption waveguide modulator/detector for optoelectronic transceiver applications," *IEEE Photon. Technol. Lett.*, vol. 8, no. 11, pp. 1540–1542, Nov. 1996.
- [66] E. Ackerman, "Broadband linearization of a Mach-Zehnder electrooptic modulator," *IEEE Trans. Microw. Theory Tech.*, vol. 47, no. 12, pp. 2271–2279, Dec. 1999.
- [67] C. Gee, T. Chen, P. Chen, J. Paslaski, K. Lau, R. Logan, M. Calhoun, and G. Lutes, "Fiber-optic link systems for antenna remoting applications," in *Proc. Photon. Syst. Antenna Applicat. Conf.*, Monterey, CA, 1993, pp. 17–20.
- [68] K. Williams, L. Nichols, and R. Esman, "Photodetector nonlinearity limitations on a high-dynamic range 3 GHz fiber optic link," *J. Lightw. Technol.*, vol. 16, no. 2, pp. 192–199, Feb. 1998.
- [69] G. Betts, F. O'Donnell, J. Donnelly, J. Walpole, S. Groves, Z. Liao, L. Missaggia, R. Bailey, K. Ray, and L. Johnson, "Microwave links using externally modulated semiconductor laser sources," in *Proc. Photon. Syst. Antenna Applicat. Conf.*, Monterey, CA, 1998, pp. 28–31.
- [70] M. LaGasse, W. Charczenko, M. Hamilton, and S. Thaniyavarn, "Optical carrier filtering for high dynamic range fiber optic links," *Electron. Lett.*, vol. 30, pp. 2157–2158, Dec. 1994.
- [71] D. Baldwin, "Dynamic range measurements comparing DFB laser links to Mach-Zehnder modulator optical links for wide-band microwave transmission," in *Proc. Photon. Syst. Antenna Applicat. Conf.*, Monterey, CA, 1993, pp. 51–54.
- [72] J. Chen, R. Ram, and R. Helkey, "Linearity and third-order intermodulation distortion in DFB semiconductor lasers," *IEEE J. Quantum Electron.*, vol. 35, no. 8, pp. 1231–1237, Aug. 1999.
- [73] K. Loi, X. Mei, J. Hodiak, C. Tu, and W. Chang, "38 GHz bandwidth 1.3 μm MQW electroabsorption modulators for RF photonic links," *Electron. Lett.*, vol. 34, pp. 1018–1019, May 1998.
- [74] J. Schaffner, J. Lam, C. Gaeta, G. Tangonan, R. Joyce, M. Farwell, and W. Chang, "Spur-free dynamic range measurements of a fiber optic link with traveling wave linearized directional coupler modulators," *IEEE Photon. Technol. Lett.*, vol. 6, no. 2, pp. 273–275, Feb. 1994.
- [75] L. Chrostowski, X. Zhao, C. Chang-Hasnain, R. Shau, and M. Amann, "Very high resonance frequency (>40 GHz) optical injection-locked 1.55 μm VCSELs," in *Proc. IEEE Int. Microw. Photon. Top. Meeting*, Ogunquit, ME, 2004, pp. 255–258.
- [76] J. Walpole, J. Donnelly, P. Taylor, L. Missaggia, C. Harris, R. Bailey, A. Napoleone, S. Groves, S. Chinn, R. Huang, and J. Plant, "Slab-coupled 1.3- μm semiconductor laser with single-spatial large-diameter mode," *IEEE Photon. Technol. Lett.*, vol. 14, no. 6, pp. 756–758, Jun. 2002.
- [77] S. Weisser, E. Larkins, K. Czotscher, W. Benz, J. Daleiden, I. Esquivias, J. Fleissner, M. Maier, J. Ralston, B. Romero, R. Sah, A. Schonfelder, and J. Rosenzweig, "CW direct modulation bandwidths up to 40 GHz in short-cavity In_{0.35}Ga_{0.65}As/GaAs MQW lasers with undoped active regions," in *Proc. 21st Eur. Opt. Commun. Conf.*, Brussels, Belgium, 1995, pp. 1015–1018.
- [78] W. Way, "Large signal nonlinear distortion prediction for a singlemode laser diode under microwave intensity modulation," *J. Lightw. Technol.*, vol. LT-5, no. 3, pp. 305–315, Mar. 1987.
- [79] S. Hwang, J. Liu, and J. White, "35-GHz intrinsic bandwidth for direct modulation in 1.3- μm semiconductor lasers subject to strong injection locking," *IEEE Photon. Technol. Lett.*, vol. 16, no. 4, pp. 972–974, Apr. 2004.
- [80] K. Lau, "Narrow-band modulation of semiconductor lasers at millimeter wave frequencies (>100 GHz) by mode locking," *IEEE J. Quantum Electron.*, vol. 26, no. 2, pp. 250–261, Feb. 1990.
- [81] D. Maack, "Reliability of lithium niobate Mach Zehnder modulators for digital optical fiber telecommunication systems," *SPIE Crit. Rev.*, vol. CR 73, pp. 197–230, 1999.
- [82] K. Noguchi, O. Mitomi, and H. Miyazawa, "Millimeter-wave Ti : LiNbO₃ optical modulators," *J. Lightw. Technol.*, vol. 16, no. 4, pp. 615–619, Apr. 1998.

- [83] M. Sugiyama, M. Doi, S. Taniguchi, T. Nakazawa, and H. Onaka, "Driver-less 40 Gb/s LiNbO₃ modulator with sub-1 V drive voltage," in *Opt. Fiber Commun. Conf.*, 2002, pp. FB6-1–FB6-4 (postdeadline papers).
- [84] W. Burns, M. Howerton, R. Moeller, A. Greenblatt, and R. McElhanon, "Broad-band reflection traveling-wave LiNbO₃ modulator," *IEEE Photon. Technol. Lett.*, vol. 10, no. 6, pp. 805–806, Jun. 1998.
- [85] Y. Chiu, H. Chou, V. Kaman, P. Abraham, and J. Bowers, "High extinction ratio and saturation power traveling-wave electroabsorption modulator," *IEEE Photon. Technol. Lett.*, vol. 14, no. 6, pp. 792–794, Jun. 2002.
- [86] K. Kawano, M. Kohtoku, M. Ueki, T. Ito, S. Kondoh, Y. Noguchi, and Y. Hasumi, "Polarization-insensitive travelling-wave electrode electroabsorption (TW-EA) modulator with bandwidth over 50 GHz and driving voltage less than 2 V," *Electron. Lett.*, vol. 33, pp. 1580–1581, Aug. 1997.
- [87] Y. Shi, C. Zhang, H. Zhang, J. Bechtel, L. Dalton, B. Robinson, and W. Steier, "Low (sub-1-Volt) halfwave voltage polymeric electro-optic modulators achieved by controlling chromophore shape," *Science*, vol. 288, pp. 119–122, Apr. 2000.
- [88] M. Oh, H. Zhang, C. Zhang, H. Erlig, Y. Chang, B. Tsap, D. Chang, A. Szep, W. Steier, H. Fetterman, and L. Dalton, "Recent advances in electrooptic polymer modulators incorporating highly nonlinear chromophore," *IEEE J. Sel. Topics Quantum Electron.*, vol. 7, no. 5, pp. 826–835, Sep./Oct. 2001.
- [89] Y. Shi, W. Wang, W. Lin, D. Olson, and J. Bechtel, "Double-end crosslinked electro-optic polymer modulators with high optical power handling capability," *Appl. Phys. Lett.*, vol. 70, pp. 1342–1344, Mar. 1997.
- [90] K. Kato, "Ultrawide-band/high-frequency photodetectors," *IEEE Trans. Microw. Theory Tech.*, vol. 47, no. 7, pp. 1265–1281, Jul. 1999.
- [91] K. Williams and R. Esman, "Design considerations for high-current photodetectors," *J. Lightw. Technol.*, vol. 17, no. 8, pp. 1443–1454, Aug. 1999.
- [92] N. Li and J. Campbell, private communication, 2005.
- [93] D. Tulchinsky, X. Li, N. Li, S. Demiguel, J. Campbell, and K. Williams, "High-saturation current wide-bandwidth photodetectors," *IEEE J. Sel. Topics Quantum Electron.*, vol. 10, no. 4, pp. 702–707, Jul./Aug. 2004.
- [94] G. Davis, R. Weiss, R. LaRue, K. Williams, and R. Esman, "A 920–1650-nm high-current photodetector," *IEEE Photon. Technol. Lett.*, vol. 8, no. 10, pp. 1373–1375, Oct. 1996.
- [95] N. Li, X. Li, S. Demiguel, X. Zheng, J. Campbell, D. Tulchinsky, K. Williams, T. Isshiki, G. Kinsey, and R. Sudharsanan, "High-saturation-current charge-compensated InGaAs–InP uni-traveling-carrier photodiode," *IEEE Photon. Technol. Lett.*, vol. 16, no. 3, pp. 864–866, Mar. 2004.
- [96] T. Ishibashi, N. Shimizu, S. Kodama, H. Ito, T. Nagatsuma, and T. Furuta, "Uni-traveling-carrier photodiodes," in *Ultrafast Electron. Optoelectron. Tech. Dig.*, Jun. 1997, pp. 83–86.
- [97] J. Paslaski, P. Chen, J. Chen, C. Gee, and N. Bar-Chaim, "High-power microwave photodiode for improving performance of RF fiber optic links," in *Proc. SPIE–Int. Soc. Opt. Eng.*, vol. 2844, Aug. 1996, pp. 110–119.
- [98] S. Demiguel, L. Giraudet, L. Joulard, J. Decobert, F. Blache, V. Coupe, F. Jorge, P. Pagnod-Rossiaux, E. Boucherez, M. Achouche, and F. Devaux, "Evanescently coupled photodiodes integrating a double-stage taper for 40-Gb/s applications—Compared performance with side-illuminated photodiodes," *J. Lightw. Technol.*, vol. 20, no. 12, pp. 2004–2013, Dec. 2002.
- [99] H. Ito, T. Furuta, T. Ito, Y. Muramoto, K. Tsuzuki, K. Yoshino, and T. Ishibashi, "W-band uni-travelling-carrier photodiode module for high-power photonic millimeter-wave generation," *Electron. Lett.*, vol. 38, pp. 1376–1377, Oct. 2002.
- [100] Y. Wu, J. Shi, J. Wu, J. Huang, F. Chan, Y. Huang, and R. Xuan, "High-performance evanescently edge coupled photodiodes with partially p-doped photoabsorption layer at 1.55- μm wavelength," *IEEE Photon. Technol. Lett.*, vol. 17, no. 4, pp. 678–680, Apr. 2005.

Charles H. Cox III (S'70–M'78–SM'95–F'01) received the B.S.E.E. and M.S.E.E. degrees from the University of Pennsylvania, Philadelphia, in 1970 and 1972, respectively, and the Sc.D. degree from the Massachusetts Institute of Technology (MIT), Cambridge, in 1979.

He is currently President and Chief Executive Officer of Photonic Systems Inc., Billerica, MA, which he founded in 1998 to provide expert consulting services in fiber-optic system design options and to develop low-cost high-performance fiber-optic links for government and commercial applications. Prior to organizing Photonic Systems Inc., he was on the research staff of MIT and with the MIT Lincoln Laboratory, Lexington, MA, as part of the Applied Physics and Applied Photonics Groups.

Dr. Cox is a member of the Optical Society of America and Sigma Xi.

Edward I. Ackerman (S'86–M'87–SM'98) received the B.S. degree in electrical engineering from Lafayette College, Easton, PA, in 1987, and the M.S. and Ph.D. degrees in electrical engineering from Drexel University, Philadelphia, PA, in 1989 and 1994, respectively.

From 1989 to 1994, he was a Microwave Photonic Engineer with the Electronics Laboratory, Martin Marietta, Syracuse, NY. From 1995 to 1999, he was a Technical Staff Member with the MIT Lincoln Laboratory, Lexington, MA. In 1999, he joined Photonic Systems Inc., Billerica, MA, where he is currently the Vice President of Research and Development.

Gary E. Betts (S'84–M'84) was born in Seattle, WA, on May 14, 1954. He received the B.S. degree in physics from Haverford College, Haverford, PA, in 1976, and the M.S. degree in physics and Ph.D. degree in applied physics from the University of California at San Diego, La Jolla, in 1980 and 1985, respectively.

From 1976 to 1978, he was with the Westinghouse Electric Corporation, Baltimore, MA, where he was involved with integrated optics, primarily on the design of geodesic lenses. From 1985 to 2002, he was a Technical Staff Member with the MIT Lincoln Laboratory, Lexington, MA, where he was primarily involved with lithium–niobate integrated optical modulators and analog fiber-optic links. He is currently a Senior Staff Engineer with Photonic Systems Inc., Billerica, where he is currently involved with microwave-frequency modulators with very high sensitivity, linearized modulators, and other high-performance microwave photonic devices.

Joelle L. Prince (M'03) received the B.S. and M. Eng. degrees in applied and engineering physics from Cornell University, Ithaca, NY, in 1989 and 1991, respectively.

From 1992 to 1994, she was a Microwave Photonics Engineer with the Electronics Laboratory, Martin Marietta, Syracuse, NY. From 1994 to 1996, she was with Micracor Inc., Acton, MA, where she developed optically pumped microchip laser technology. From 1996 to 2000, she was with the MIT Lincoln Laboratory, where she was involved with analog photonic links for microwave communications and antenna remoting applications and wavelength-division multiplexing (WDM) optical communication networks. From 2000 to 2003 she was with AXSUN Technologies, Billerica, MA, where she developed optical spectral analysis equipment for WDM optical communication networks. She is currently a Principal Engineer with Photonic Systems Inc., Billerica, MA.

